Cerebral Blood Vessels Modeling

Anna Puig Puig

1 Introduction

The computer-aided reconstruction of anatomical structures from a set of 2D images such as Computer Tomographies (CT) and Magnetic Resonances (MR) is becoming an important aspect of the medical diagnosis and the surgery simulations. Vascular diseases, which are around a 10% of the clinical examinations, are complex to analyze because vascular structures are small and narrow. The new input technologies enhance their study.

In this report, the reconstruction and modeling of cerebral vascular structures are addressed. The main contributions brought are the following:

- A representation scheme of the cerebral blood vessels, based on the three-levels conceptual modeling process: physical, mathematical and representation ([Man88]). The symbolic model provides representation of both the surface of the vessels and their internal volumetric properties. These properties are the tissue density, the blood flow velocity and the vessel wall elasticity, which are specific of the vascular structure. The model is evaluated in relation to the operations that neurosurgeons perform in the clinical routine.

- The algorithm of construction of the model from data obtained using the vascular registration techniques. The algorithm is based on a seed strategy which analyzes the characteristics of the blood vessel MAT (Medial Axis Transform), its regular features as well as its anomalies. It recovers the information of the semantics, of the topology, of the geometry and of the volume of the vascular map from an input discrete representation.

This report begins with the presentation of the background on the blood vessels modeling and visualization in section 2 where the practice on the diagnosis of vascular diseases (2.1) and the medical issues on computed-assisted diagnosis (section 2.2) are explained along a survey on the previous work on this topic (section 2.3) are explained. In section 3 the cerebral blood vessel representation scheme is defined; the operations are described and the model is evaluated in relation to the specifications of [Req80]. The algorithm of the model construction is proposed in section 4. Finally, the conclusions and the future work are presented in section 5.

2 Blood vessels modeling and visualization: Background

2.1 Diagnosis in the cerebral vascular map

2.1.1 Brief description of the anatomy

The cerebral vascular system is a tree of blood vessels, veins and arteries, which irrigate the Central Nervous System. These two types of vessels have similar and asymmetrical paths. While in the arteries, more elastic, the oxygen concentration is high and the blood flow is abundant, in the veins, more rigid, it is the CO_2 concentration which is high and the blood velocity is low. This difference makes the data registration more accurate in the arteries than in the veins.

The diameter of the vessels, which is of 1 cm in the carotids, becomes narrower in the branchings, reaching 0.5 cm in the small arteries and about 0.001 cm in the microcapilars.

In each vessel, two regions may be defined, the inner one, where the blood flows, and the vascular wall or parenchyma.

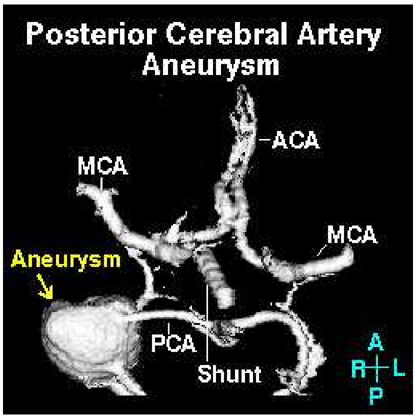

Figure 1: Cerebral Aneurysm.

There are two types of frequent vascular accidents which occur with death consequences in about a 5% of the more than 65 years-old population: haemorrhages and embolysms. Haemorrhages are produced by vessel ruptures due to a local growth of their diameter, called *aneurysm* or venoma. These dilations are caused by a increase in the local elasticity of the wall. Embolysms and thrombosis are obturations of the vessels as a consequence of a progressive narrowing of their diameter, or *stenoses*. These vessel constrictions may be produced by pressions of external structures such as tumors or by sedimentation of the blood.

In order to prevent these diseases it is necessary to realize early diagnoses of aneurysms and stenoses before the apparition of further complications. The prevention enables the use of pharmacological treatments and even surgical interventions such as prosthesis implants.

2.1.2 Diagnosis Techniques

The properties most used by physicians in order to diagnose vascular accidents are:

- *Blood vessel Morphology:* The shape and the interrelationships between blood vessels are the basic information in order to detect eventual anomalies.
- *Diameter:* The diameter of the vessels cross-sections is used to detect malformations.
- *Velocity:* Differences in the blood velocity at several points are measured in order to find stagnancy regions.
- *Blood pressure:* The pressure of the blood, related to its speed, enables to detect hypertension in obtrusion zones.
- *Elasticity:* The elasticity of the vascular walls may indicate dilations or sedimentation.

The input techniques more frequently used are:

- Digital Subtraction Angiography (DSA): technique similar to the radiograph, which consists of capturing two consecutive image projections of the patient: before and after the injection of a contrast agent. It enables to obtain information on the morphology of the vessels.
- Magnetic Resonance Imaging (MRI): technique based on the behavior of the mono-protons and mono-neutrons atoms in a magnetic field. It registers the average density of the stationary tissues around a point, thus giving information of the parenchyma. As it does not work with an absolute scale of values, it gives a lot of segmentation problems.
- Magnetic Resonance Angiography (MRA): Technique similar to the MRI, which removes the signal produced by stationary tissues and which detects the presence of fluids. It registers the average density around a point of the fluid, giving therefore direct information of the intravascular region. Two types of MRA exist: *Phase-Contrast* (PC) and *Time-Of-Flight* (TOF). The PC technique gives the density as well the internal velocity in the vessels while the TOF registers only the presence of the flow. Although the latter one is faster than the former one, it requires the acquisition of complementary information.
- Spiral Computed Tomography Angiography (SCTA): technique based on the interpolation of X-Rays data. After a contrast agent injection, the head is scanned in spiral with x-rays. The SCTA captures the density around any point of the head.
- Doppler: the Doppler is used in order to obtain data of the blood speed at lower cost. It measures the speed at some user-specified points from which the blood velocity at other locations can be extrapolated. The Doppler

combined with ecographs allows the computation of data related to the acceleration and of the maximum and mean blood velocity along with the elasticity at given points of the vascular structure.

The arteriographs and the DSA present the main drawback of producing planar projections of anatomical structures and of reducing the diameter of the blood vessels, loosing information of the very tiny and narrow vessels. Although several methods have been developed to reconstruct the three dimensional model from two projections [FR92], [GCCC91], [KTS88], [SFTPR90], some ambiguities appear on the 3D topology due to the complexity of the vascular structure.

MR and CTSA techniques give instead a set of regularly sampled cross-sections of the anatomical structures. They provide a natural mean to reconstruct the 3D model. This is the reason why, although they are more expensive, they are generally preferred for 3D modeling. In the remaining of the report, only these techniques will be addressed. The data are sets of around one hundred 256x256 or 512x512 images, spaced 1 mm with an approximate resolution of 0.1 mm and 12 bits of property value.

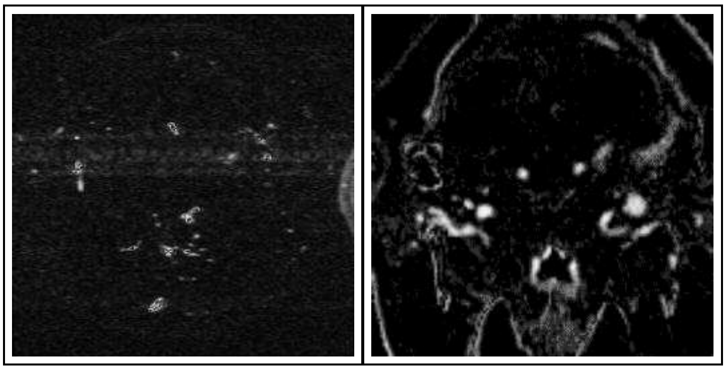

Figure 2: Behavior of MRA and SCTA values, respectively.

The behavior of the density values are depicted in Figures 2. Both techniques are evaluated in table 1 according to: the sampled property, the contrast between blood vessels and parenchyma, noise sensibility and loss of signal caused by slow flux and turbulences, harmfulness of the techniques.

	MRA	SCTA
Properties	density and velocity	density
Contrast	Low	High
Noise	High	Low
Loss signal	Yes	Yes
Harmfullness	No	Yes

Table 1: Evaluation of MRA and SCTA tecniques.

The images generated by the MRA techniques have a low contrast and they have noise in high levels of intensities due to the magnetic susceptibility to artifacts, to heterogeneous RF fields and to variations of sensitivity of the receiver antenna. In addition, in high intensity vessels smaller than one voxel width, the signal is lowered by the neighbor tissue, reducing thus their contrast. Furthermore, the signal may get lost when the flux is too slow or when a turbulence appears. Therefore, the MRA intensity values of interior voxels of a blood vessel do not belong to a given range of values but they are higher than the neighbor values. It should be noted, however, that some local maxima can be produced by high intensity noise. The main MRA advantage is the capability, in PC-MRA, to capture the velocity of the flux although the capture time is multiplied by four.

The SCTA images are very contrasted because of the injected agent and thus the values of density exhibit large differences. As above, some losses in the signal may appear due low flux and turbulences. The main drawback of this technique is that it is harmful and it may have secondary effects on the patient.

On the basis of the images and the computed values, physicians mentally reconstruct the 3D vascular structures in order to detect injuries. During this process, the regular anatomical structures guide the detection of pathological formations, which are found by successive approximations of the measurements. This mental process is very hard because of the complexity of the cerebral vascular system and the low ratio between the vessels and the brain (about a 20%).

2.2 Computer Assisted Neurovascular Medicine

The main goal of a neurovascular software application is to assist the physician in its diagnoses and surgical planning. First, as mentioned above, several input devices are not able to measure properties such as velocity. Thus, these properties must be extrapolated by, for instance, simulating the blood flow. In the *educational* field, the visualization of the structure and the possibility to virtually operate on the vascular map provides the mean of a better understanding. In order to make more accurate *diagnoses*, the specialist should have the possibility of visually exploring the vascular tree either isolated or integrated with the brain, with different levels of precision and with access to property values, such as density, flux, pressure and diameters. In addition, an *automatic detection* of vascular accidents is desirable. The interactive navigation through the vascular tree is required for the *surgical planning*. Finally, the *prediction* of vascular accidents should be enabled on the basis of a given aging model.

Summarizing, the requirements of a neurosurgical application are:

- *The reconstruction of the cerebral vascular tree:* all the 3D information implicit in the input images property values should be recovered and interpreted in order to construct a 3D model.

- *Visualization of the vascular map:* the visualization of the internal volume of the vascular tree, density values and velocity vector fields, should be enabled, separately from the vessels surface display or in an integrated way. Changes in the light source positions and intensities, in the viewpoint position and zooming must be interactive.

- *Interactive navigation in the vascular map:* The system should provide means of changing the viewpoint along with an interactively defined path through the vascular structure and of displaying the local views of the vessels surface and their internal volume.

- *Detection of vascular accidents:* The automatic detection of points of the vascular map with pathologies such as aneurysms and stenoses should be allowed.

- *Integration with the brain.* The vascular model must be fitted into a more general representation of the brain.

- *Measurements:* The model should allow measurements of the vessels diameters, of cross-sections areas and of the blood pressure and the elasticity of a vessel.

- *Blood flow simulation* The model should allow efficient computations of the blood flux in any segment of the vascular tree.

- *Flux prediction:* Given an aging model, the new velocity of the blood flow may be predictable and its storage in the model should be enabled.

2.3 Previous work

As MR and SCTA are particularly suitable for the registration of the blood vessels, the previous work surveyed herein focus at these type of data. Two main strategies have been proposed in computer assisted neurosurgery systems: direct visualization of the data and reconstruction of the vascular map.

Direct visualization methods

By opposite to other structures, the ratio between vascular information and surrounding data is very low. Thus, single MRA and SCTA images provide very little data of the 3D vessels anatomy. Therefore, the whole set of images must be displayed simultaneously [CP92].

In order to obtain quality images, a segmentation process is required, either previous to the visualization or inserted in the classification. In [CLKJ90] the Phase-Contrast segmentation is performed during the acquisition stage in order to isolate the vascular structure from the stationary tissue. In most cases however, the segmentation is performed on the images, after their capture. The MRA images present low error signal and heterogeneity in the intensity. Several segmentation algorithms on these type of images have been specifically designed for the detection of small structures of low contrast and narrow objects causing signal attenuation. The algorithms take into account the photometric properties of the data ([HTL+89]), the shape of the blood vessels ([GKJ90], [EDKS94]) and the continuity of the vascular map ([GKJ90]), [VVM+93]).

[HBP+90] uses the *Transparent Greylevel Gradient shading* (TGG) without realizing a previous segmentation. Therefore, as the TGG depends on the density property value, the quality of the images is low around small vessels. In general, any shaded visualization on segmented data may be suitable as far as the shading is based on a property value adequately sampled on the object (this is not the case of the density value on MRI data for instance). Shaded visualizations, however, are slow for interactive medical diagnoses. Their speeding up using 3D SGI texture mapping and back-to-front projection of pre-segmented, pre-classified and pre-shaded models is under study [Zui96].

The Maximum Intensity Projection (MIP) [GS95] does not require a segmentation pre-process, although it can be improved by it [SVD+91]. MIP takes advantage of the fact that, due to the capture process, data corresponding to vessels have a higher intensity than the surrounding regions. Therefore, by projecting the maximum intensity found in each ray, MIP outlines the global vascular structure. However, as pointed out in [EL90], this visualization lacks depth perception and it is sensible to noise. Therefore, it has the same disadvantages as DSA and X-Rays images: ambiguities in the overlapping of vessels, diameters reduction and loss of the smallest vessels. Some of these drawbacks may be avoided by adding depth clues to the rendering [HMS95] but MIP still cannot provide a perception of the whole 3D vascular tree in a single image. In addition, although several methods have been proposed in order to speed-it up [GS95], MIP is computationally expensive: in practice, several different MIP views are computed in batch and recorded as a film for clinician's use.

Vessel reconstruction

The vessel structure reconstruction methods fall into two categories: that which attempts to extract the vessel surface from the data and that which constructs a symbolic model of the vascular tree, from which a simplified approximated surface model may be computed. Both cases require the binary segmentation preprocess cited above.

The narrow tubular structure of the vessels poses numerous problems for the surface extraction. Marching Cubes (MC) [GKJ90] and Dividing Cubes (DC) [CLKJ90] algorithms may skip over small vessels and generate a huge amount of polygonal faces. According to [EDKS94], the trilinear interpolation done in these methods is not suitable for the modeling of local deformations in elbows, aneurysms and stenoses.

The most revelant symbolic approaches are:

- In [BGSC85] a symbolic model of individual vessels was early proposed, composed of cylinders joined onto common circular sections. The model was extracted by manually sampling points along the vessel axis and measuring the thickness of the vessel there.

- In [ZJP94] an algorithm for the automatic extraction of a symbolic tree of the vascular structure is proposed. The tree is composed of numbered branches connected at bifurcation nodes, where the diameters of the vessels and the axes orientations are stored. The voxels interior to the vascular tree are labeled with the number of the branch to which they belong so that they can be projected and colored separately. No surface reconstruction is proposed from the symbolic model, although it is feasible.

- The model automatically computed in [EDKS94] is a tree of spline curves marking the center lines of the vessels, plus a sequence of cross-section contours perpendicular to the axis. A smooth surface model composed of tensor product rectangular patches can be bounded on this symbolic model.

- [WW97] produces an abstract model of the topology and geometry of the tree as a connected network of tubes and balls, using local operations based on morphology and on differential geometry. They extend a previous method ([WHH+93]) which obtains the axis using a 3D seeded region growing algorithm based on differences in CT number between wall and lumen. As this segmentation process gives poor results, [WW97] find the directions of extreme curvature for determining the optimal plane which intersects the vessel structure in order to accurately measure the centroid and the cross-sectional area.

- [GKS+93] extends to 3D, a 2D parallel thinning algorithm enabling a construction of a medial line of one-voxel width. They apply a vectorization algorithm based on lambda-shape from which an abstract graph model is constructed, composed of cylindrical pieces united at bifurcations.

Evaluation

Systems based on direct visualization of the volume data allow almost interactive visualizations, enabling the visual understanding of the 3D structure of the vessels integrated with the brain and of their pathologies. However they are not able to provide real-time walkthroughs in the vascular structure, and to give direct measurements of the diameters. They are not either suitable for the blood flow simulation and prediction.

Characteristics	[Bar85]	[ZJP94]	[EDK94]	[WiW97]
Adquisition	Steroscopic X-Ray	SCTA	MRA i SCTA	CT
Model	Cylinder set	Label tree	Spline axis and Cross-sections	Tubes and balls network
Building Method	Manual	Seed	Seed	Morphology
Visualization	Surface	Volume	Smooth surface	Simbolic
Navigation	No	No	Via hardware	No
Feature vessels	Regular	Regular and branchings	Regular and branchings	Regular and branchings
Brain integration	No	No	Yes	No
Mesurements	Diameter	All diameters	Feasible	All diameters
Fluid simulation	No	No	No	Yes
Prognosys	No	No	No	No

Table 2: Analysis of symbolic model methods.

Modeling techniques, instead, allow real-time navigations, recognition of the 3D structure and its pathologies, direct measurements and blood flow simulation and prediction. The integration of the vascular model with a model of the brain is possible although it is much more difficult than in the visualization approach.

The construction of a symbolic model of the vascular tree presents several advantages over the first approaches exposed. First, it provides by itself a good understanding of the structure. Next, it may allow the generation of a simpler and smoother surface model, therefore suitable for fast interactive visualizations, navigations and flow simulations. However, as pointed out in the cited references, this approach encounters several problems: axes and bifurcation detection, diameters computation.

The table 2 synthesizes the methods that use symbolic models and it evaluates them versus the surgeons requirements, defined in the section 2.2. They present two main drawbacks: first they do not provide an identification of the vessels anomalies and next they do not integrate the surface and the volume information. The model proposed herein is intended at fulfilling these gaps.

3 Modeling of blood vessels

The main goal of modeling in medicine is to provide 3D representation schemes of anatomical structures and algorithms suitable for their manipulation.

Following the methodology proposed in [NPT93], the three main modeling steps are next derived: (i) characterization of the physical model of the medical objects that should be represented and of the operations that should be performed on them; (ii) definition of the mathematical model and, (iii) evaluation of the most suitable computational representation scheme.

3.1 Physical model

The physical model characterizes the cerebral vascular map morphology and it defines the properties to be analyzed.

The cerebral vascular system is a tree of blood vessels with multiple branchings. Although, in some malformations, isolated vascular structures may exist, in general, it can be assumed that the cerebral vascular map is a connected structure. It is a finite area object, this is, it has a boundary of closed area and continuous in C^0. In addition, it does not have any hole and its inner region is path-connected and two-manifold.

Depending on the shape of the vessels cross-sections and on the variation of the area along the main direction of the blood flux, two types of vessels may be distinguished: regular vessels and abnormal vessels. It is supposed that the cross-sections of the vessels in which the area is measured and the shape of the section is evaluated, are perpendicular to the main direction of the flux. The following taxonomy synthesizes the possible shapes of vessels:

- **Regular** segment: segment of a vessel such that it is a tubular, narrow structure, connected, smooth and without skretching, with approximately circular or elliptical cross-sections ([FR92]). The diameters of the cross-sections of these regular vessels vary linearly, either increasing or decreasing.

- Stenoses or **constriction**: segment where it exists a local minimum in the area differential along the vascular axis. This definition encloses both asymmetrical and symmetrical stenoses.
- Aneurysm o **dilation**: segment where it exists a local maximum in the area differential along the vascular axis. Similarly to stenoses, aneurysms may be symmetrical or not with regard to the main flux direction.

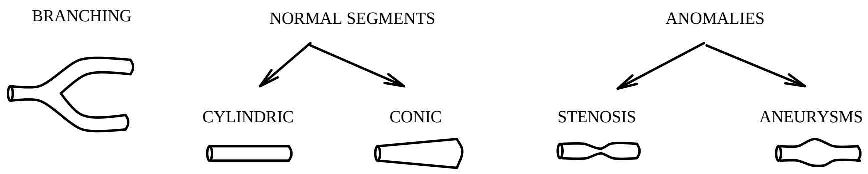

Figure 3: Typification of the characteristics to be modeled.

Points in the vessels boundary have information on the elasticity and the density of the vascular wall. Points which are interior to the vessels have information on the blood flow: viscosity, pressure and velocity of the blood.

External points belong to the cerebral parenchyma. Several anatomical structures delimited by a continuous surface boundary, such as the encephala, may be defined in the parenchyma. However, for the vascular applications, it is sufficient to consider the density values associated to the external points without further distinctions on the anatomical structure to which they actually belong.

3.2 Mathematical model

The mathematical model of the vascular structure is naturally a graph $G(n, e)$ such that n are the nodes of the graph which represent the branchings of the vascular map and e are the edges between branchings, composed of a set of segments either normal or abnormal.

Def. 1. The **symbolic vascular model** is defined as a 7-tuple $< V, E, T, \Sigma_{etiq}, \delta, I, F >$ such that V is the finite, and non-empty set of nodes, T is the set of anatomical features, and E is the set of edges, each of them composed by a concatenation of anatomical features, such that:

$$
\begin{array}{rcl}
E & \in & V \times V \\
E & = & \{e \ / \exists n : n > 0 : \forall i : 1 \leq i \leq n : concat_{a_i \in T}(a_i) = e\} \\
\Sigma_{etiq} & = & \{Branching, Normal, Aneurysm, Stenoses\} \\
\delta & : & T \rightarrow \Sigma_{etiq} - \{Branching\} \\
 & & V \rightarrow \Sigma_{etiq} - \{Normal\} \\
I & \in & E \text{ Initial edges of the graph} \\
F & \in & E \text{ Final edges of the graph}
\end{array}
$$

where,

$$concat_{a_i \in T}(a_i) = a_0 \cdot a_1 \cdot a_2 \ldots a_n, a_i \in T$$

is the set of anatomical features of the vessels ordered along its axis.

In the previous physical model analysis, it has been shown that boundary points and interior points have different associated data. Therefore, the mathematical models of the boundary and of the internal volume represented at the edges and at the nodes of the graph are next presented separately.

3.2.1 Mathematical model of the boundary surface

Since the physical structure of the object is tree-like, an abstract tree with nodes representing junctions and edges representing tubes presents itself as the obvious choice for the logical definition of the vascular area.

Blood vessels may be considered as closed objects resulting from a cylindrical sweep in which there are no intersections neither in the contours nor in the profiles. Therefore, the mathematical model of the vascular map surface is based on the following definition of Generalized Cylinders.

A *Generalized Cylinder* is an axis curve which defines the sweep trajectory, $SKLT(t)$, a set of arbitrarily shaped cross-sections, $C_i(t)$ and a set of *blending* functions between consecutive sections, $Bl_i(t)$. In the blood vessels model the *blending* is not taken into account because the physical model does not present twists on the shape of the vessels.

A *Generalized Cylinder* is defined as the union of the contour curves $S = \bigcup_{a \leq u \leq b} C(u)$ or the union of the profile curves $S = \bigcup_{0 \leq v \leq 2\pi} SKLT(v)$ such that:

- The skeleton curve, $SKL(t)$, is continuous.
- Each section in the normal plane of the main flux direction is a closed curve, $C_i(t)$, with a reference point, p_i of the skeleton curve.
- Any $C_i(t)$ has a one-to-one correspondence with a circle of radius 1, centered in the point p_i of the plane, such that if a ray is traced in the plane from p_i to any point of $C_i(t)$, this line only intersects once the unit circle.
- $SKL(t)$ does not self-intersect, i.e., it is homeomorphous with a line.
- The generalized cylinder obtained with the axis $SKL(t)$ and the set of contours $C_i(t)$ guarantees that the surface does not self-intersect, i.e. $\forall p_i$ $radius_{curvature}(SKLT(t)) > radi_{maximum}(C_i(t))$.

Therefore, the mathematical model of the vascular map surface is defined as the union of generalized cylinders ([KPL94]) which represent each segment of the tree.

3.2.2 Mathematical model of the volume

The more general abstraction that can be done about volumetric attributes is that a volume is a set of points in the 3D-space with values corresponding to the different physical properties. This abstraction leads to the Point Topological Model [Man88] which is general and which can represent any object.

From the cerebral vascular analysis, the basic properties are the density and the blood velocity. From them, any vascular region and any other physical property can be defined. The blood pressure may be derived from the velocity and the vessel diameter. The elasticity can be computed from the density. The values of these properties are characterized by functions which behave differently depending on their domain and the area in which they are defined.

Therefore, the vascular model, MVV, is characterized by all the property functions for all the properties which characterize the object [NPT93] in a region R of $\Re^3$:

$$MVV(R) \quad = \quad \{j \in \{density,\ velocity\} \ \&\ (x, y, z) \in R \ / f_j(x, y, z)\}$$

The **density** is a scalar value that defines different homogeneous regions of the encephalic structure: skull, encephala and vascular map. It is defined with a function den continuous in C^1 which varies linearly in each homogeneous region. It is thus assumed that a boolean segmentation function $f_{seg}(den(x))$ allows to determine if a value of density is internal to the vascular region.

The velocity is a 3D vector value that differenciates two homogeneous regions: the area where it is zero is the parenchyma and the area where its value is non-zero is the intravascular region. This distinction is a simplication of the physical model because, in the intravascular region, some turbulences may give zero values of velocity as well. The velocity function vel is C^1 continuous.

As shown in Figure 4, the velocity can be defined parametrically $C_i(t)$ with the central density value. The main direction of the flux is the resulting vector of the velocity vectors in a cross-section perpendicular to the vascular walls in a point. In a regular segment, the main direction is perpendicular to the section plane $C_i(t)$.

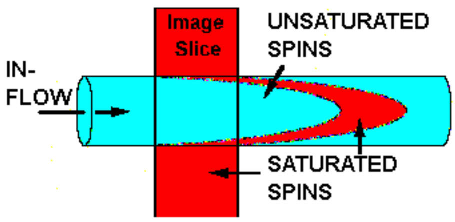

Figure 4: Velocity in a cross-section of a vessel. (Image from http://www.xray.ufl.edu/ rball/flow.html)

Finally, depending on the segmentation function, f_{seg} and on the density (den) and the velocity values (vel), the following regions of a blood vessel should be considered:

- Internal region: set of points which belong to a given neighbourhood of the vascular axis e, $dist(e, x)) \leq \delta_{ri}$ and $vel(x) \neq 0$ and $f_{seg}(den(x))$, being δ_{ri} the internal radius of the vessel.

- External region: set of points which belong to a given neighbourhood of the vascular axis $\delta_{ri} \leq dist(e, x)) \leq \delta_{rext}$ and $vel(x) = 0$ and $not(f_{seg}(den(x)))$, being δ_{rext} the external radius of the vessel.
- Vascular boundary: set of points of the internal region such that, for any given neighbourhood, at least one point of the external region may be found.

3.3 Operations on the model

According to the requirements of the applications described in section 2.2, the basic operations that should be performed on the model are: the construction of the model from a set of images, the visualization of the model, the reconstruction of the vascular surface, the navigation, the automatic detection of vascular accidents and the property measurements.

3.3.1 Construction of the model

The **construction of the model** is done from a set either of MRA, SCTA or Doppler images, which stacked altogether compose a voxel model. This model contains data of the density and the velocity within a bounding volume of the vascular map. As mentioned above, other vascular properties are derived from the density and the velocity.

The data are segmented using the methods previously described, rather complex for MRA, given its density values distribution([VVB+94]), and simply based on threshold values for SCTA. The segmentation produces a binary volume which indicates the presence of a blood vessel.

It is supposed that the discretization of the blood vessel surface after the capture and the segmentation is as follows:

- **binary**: any voxel v with a 1 value belongs to the vascular structure EV.
$$\forall v \ : \ value(v) = 1 \Rightarrow v \in EV \tag{1}$$
- **wrapping** in relation to the vascular surface SV, i.e., any voxel crossed by the surface belongs to the 1 values region:
$$\forall v \ : \ SV \cap v \neq \emptyset \Rightarrow value(v) = 1 \tag{2}$$
- the voxels of boundary of the vessels are **26-connected** and the width of this boundary is at most **two voxels**.
- such that a 0-value voxel always exists between two different blood vessel.

The tree former hypotheses are arbitrary, independent from the original data, done just for convenience. The fourth hypothesis about the minimum distance between two neighbor vessels is necessary in order to extract a unique valid model of the vascular tree. Otherwise, the ambiguities of the data would lead to various possible solutions which are useless for the physicians. This hypothesis thus is a rather reasonable requirement for the data capture to provide enough resolution.

3.3.2 Visualization

Different types of **visualizations** should be performed: of the vascular map surface, of the internal volume properties, hybrid surface-volume and integrated with the parenchyma either with an opaque or transparent boundary display.

The visualizations should enable:

- the perception of the vascular topology, its features, such as stenoses, aneurysms and branchings as well as the relationships between these features.
- Tridimensional perception of the structures
- Tridimensional perception of the vascular surface
- Interactivity
- Zooming of interest areas
- Different levels of quality and detail
- Adaptability to hardware accelerations

3.3.3 Other operations

In order to evaluate the surface of the vascular map, the model should allow the **reconstruction** of the vascular surface from the information stored. This surface will enable to do interactive visualizations, walkthrough and it will be the basis of the blood flux simulations. This is reason why it may be necessary to reconstruct the surface at different levels of detail according to the operations that should be performed.

All types of **Navigations** through the model, either visualizations or fluid simulations, should be enabled. The visual navigations through the internal region of the blood vessels must show the surface boundary and the internal property values. In the external areas, the relationships between the vascular map and the encephala must be outlined allowing boundary transparency. The fluid dynamics simulations also require navigations through the model in order to access to the points in which property values are simulated.

The **vascular accidents** must be automatically detected and represented with different levels of accuracy and detail.

Sections of the model by any plane must allow the clipping of interest areas.

Several **measuraments** must be allowed: either interactive or non-interactive queries to any property value on a point, along with area and volume computations.

Topological and connectivity **queries** on the representation scheme must be enabled, along with global queries such as the number of anomalies and the total volume of the model.

3.3.4 Conclusions

For any point of the internal region of the vascular map, it is necessary to know the following data: its position, the region to which the point belongs, either intravascular or boundary, the diameter of the section of the vessel at the point, perpendicular to the blood flow; the set of properties associated to the point and the path from the point to any other point of the vascular map.

For any external point, the density value of the parenchyma may be computed.

In addition, the representation model should enable to represent the surface at different levels of details, giving, at any level, the coordinates of any point, its surface normal and its density.

3.4 Representation scheme

From the mathematic model presented in section 3.2, the representation scheme is defined as a graph such that its nodes are the branchings and its edges are the connections between branchings. Each edge is subdivided into segments labeled as the different features: normal, stenoses and aneurysm. Every node and edge of the graph has associated both surface information and volume data of the vascular map. According to the requirements exposed above, it is therefore a hybrid symbolic model which labels the different vascular features. It defines the blood vessels topology and it identifies explicitly the connectivity and the different features.

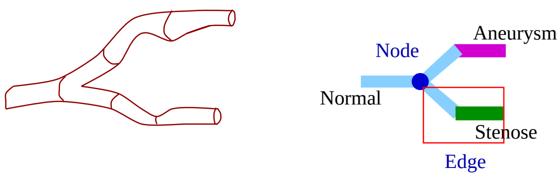

Figure 5: Representation scheme

The surface and volume information stored at the nodes and the edges of the graph are next detailed separately. Then the interrelationships between both types of information are defined.

3.4.1 Surface representation

The vascular surface models proposed in the bibliography can be classified into two groups: cylindrical approximations ([BGSC85], [GKJ90]) and smooth surfaces such as biquadratic splines ([EDKS94]). In the former case, the segments are represented implicitly by their radii and centers. The memory requirements are thus low, while the visualization can be fast because most of the 3D graphic libraries enable a hardware-driven visualization of cylinders. This representation however is not adequate for the modelization of aneurysms, stenoses and branchings. For these features, a smooth surface approximation such as the one proposed in [EDKS94] is more convenient, although it requires more memory.

In addition, not all the operations on the model need such a level of detail in the representation.

In most of the literature of solid and surface modeling, generalized cylinders are represented as the profile curve and the contour curves associated to different section of the profile ([Ros85]). These curves can be approximated with different precision as polygons or B-splines [MPSY97]. The number of contour curves stored must be sufficient to interpolate any intermediate curve without loosing continuity.

Therefore, the surface model proposed herein is defined parametrically. It associates to each node of the graph ω and to each segment T of the graph edges a set of information which can be interpreted in different ways enabling thus various level of details of the surface.

The superficial information is a set of sections across the central axis of the vascular structure or skeleton curve such that:

- The skeleton curve is simplified as a set of points which guarantees that it is C^1 continuous.
- Each section of the generalized cylinders is defined by a Frenet Frame.
- Each section of a Generalized Cylinder is represented as a set of points which approximate the contour curve at different levels of precision, from a simple polygon, a circle, an ellipse, to a spline.
- It is sufficient to store sections only at points of the skeletal curve where a significant change of curvature or diameter exists and at end-points of the different features.
- There is a unique correspondence between the points of two consecutive sections. In the branching nodes, this correspondence is based on the criteria defined in [Boi85] and [AOUK87].
- The variation of the surface between two consecutive cross-sections may be linear or can be represented by smooth patches C^1 continuous according to [KPL94].

In regular segments, the most simplified contour information is represented implicitly because the sections are circles and thus, it is enough to store their diameters. In addition it is supposed that, in these segments, the diameter varies linearly. Therefore, in a cylindrical segment a single diameter for the whole sweep curve is sufficient. In a conical segment the initial and the final diameters are stored.

This surface representation enables to evaluate the geometry of the boundary model with different levels of detail. The simplest evaluation is a simple union of cylinders between nodes. A smoother one consists in polygonalizing the surface by tiling between contour curves. Finally, it can be approximated by biquadratic rectangular splines.

The multiresolution of this model is suitable to the variety of operations that must be realized on it. Some operations, such as fluid simulations, require only simple cylindrical approximations while other ones, such as the navigations, need smoother surfaces.

3.4.2 Volume Representation

The voxel model of the cerebral vascular map is defined from its bounding box and not from the bounding box of the whole brain. Even though, considering the sparse structure of the vessels, the voxels corresponding to the vascular map occupy only around a 20% of the model. Thus, the voxel model seems to require too much memory to be suitable for the representation of the vessels. Several compression schemes have been analyzed in the literature [BJN+94], such as the octree model and the frequencial models but the interrelationship with the surface is complex. The model proposed herein compacts the voxel model using a run-length encoding [Lac95], [HL79].

The initial voxel model has been previously segmented and each voxel stores a simple identifier of the segment of the tree to which it belongs. This identifier defines a new volume property of ownership of each voxel to a segment of the tree structure. The model is compacted by a run-length encoding method on the basis of this property values.

Moreover, in order to keep the different property values of all the interior voxels of the vascular structure, for all the segments of the graph nodes and for all the branches, a subset of the original voxel model enclosing the segment is stored. This subset run-length encodes the property values only of the voxels which belong to the segment. This is depicted in Figure 6.

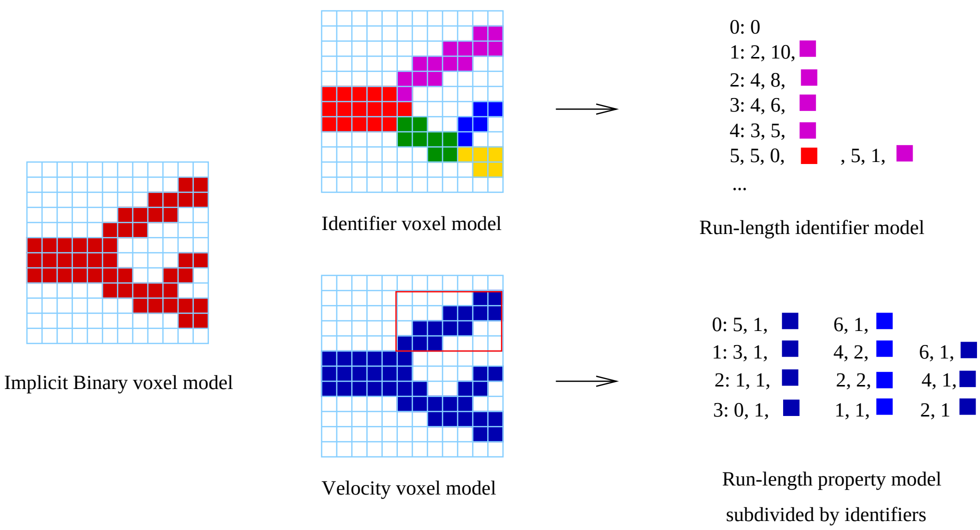

Figure 6: Run-length encoded volume model

This doble structure (encoding of segments and branches and encoding of the property values) enables to take advantage of the spatial structuring of the voxel model. Thus, it allows a direct access to the property values of any voxel of a segment or a branch. In addition it enables to design culling algorithms for the compressed model similar to those used in the Shell representation scheme [Udu92] along with fast internal volume navigations.

3.4.3 Hybrid representation scheme

The interrelationship surface-volume guarantees that, for any surface point it is possible to access to its corresponding voxel using its coordinate values and, accordingly, there is a direct identifier to the segment of the graph to which any voxel belongs.

3.4.4 Model evaluation

The representation scheme defined is:

- Complete: It represents a connected tree-like structure and it codifies different property values (density, diameters and velocity) of different type (scalar or vector). These properties may be consulted and modified in any internal point of the vascular map. In addition, the model contains explicit information on the vascular accidents.
- Valid
- Non ambiguous
- Finite: The region of space and the set of properties represented are discretized into a finite number of elements.
- Multiresolution: It allows several levels of detail in the surface reconstruction from the information stored. It has two levels of detail for the volume: the simple label and the full-resolution volume properties.
- Hybrid: It contains information on the volume and on the surface. The interrelationships between the surface and the volume are set in the model in such a way that from the surface of a vessel the property values are accessible and from a boundary voxel the surface properties are retrievable. In addition it is possible to access to the encephala data.

This model enables directly the realization of some requirements listed in section 2.2: reconstruction of the cerebral blood vascular tree, detection of the vascular accidents and measurements. The blood flow simulation and the flux prediction are possible because the model provides the vascular surface. The visualization and the interactive navigation can be performed according to different strategies as exposed in [Pui98b].

4 Construction of the representation scheme

In this section the construction of the proposed model from a set of previously segmented images is addressed.

Characteristics	Graph	Surface	Volume
Connected structure	×		
Tree structure	×		
Surface-volume integration	×	×	×
Properties		Diameter	Density and velocity
Visualization	Hybrid	Cylinders and spheres Smooth surfaces	Shaded rendering
Navigation	×		
Feature vessels	×	Geometry	Volume
Brain integration			×
Mesurements		Diameter	Volume
Topological queries	×		
Fluid simulation	×	×	×
Prognosys	×	×	×

Table 3: Model evaluation with regards to the requirements and the operations

4.1 Problem analysis

Reconstructing the symbolic model with the surface and the volume associated to it consists mainly in detecting the features of a skeletal representation of the vascular map. The skeletal representation used is the Discrete Medial Axis (DMAT), defined in [Pui98a]. Although many other definitions of discrete objects skeletons exist, such as those produced by thinning algorithms [LK94] and mathematical morphology [MMD96], these skeletons do not reflect in their geometry the information of the different features that should be detected. (see Figure 7). This is the reason why the DMAT, which is a complete, continuous and valid model, is preferred.

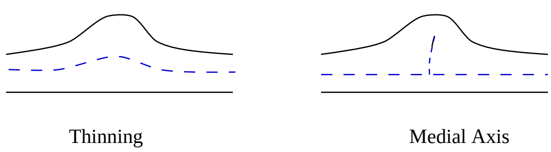

Figure 7: Thinning and Medial Axis skeletons of a feature.

4.2 General strategy

The construction of the blood vessel model, i.e. the graph defined in section 3.2, involves two different tasks: first the computation of a discrete skeleton of the blood vessel surface, and next the identification of the nodes, features, sections and internal vessel voxels of the model along with their topological relationships from the analysis of the discrete skeleton.

In order to reduce the cost of the algorithm and to perform both processes simultaneously, a single-pass seed strategy has been proposed.

Although the two processes are performed simultaneously in a one-pass strategy, for clarity they are explained separately in this section.

In the next sections, the three steps of the second pass are exposed separately. These steps consist respectively in the retrieval of the semantic and topological information of the model (symbolic model), the construction of the geometry and the topology of the surface (surface model) and finally the construction of the internal property values (volume model).

4.3 Algorithm of construction of the symbolic model

The construction of the symbolic model is based on the fact that the Discrete Medial Axis Transform of the discretized vascular map reflects the shape of the surface. Therefore the algorithm consists mainly in detecting the features of the MATD. It is next shown that this detection is based on the typology of the points that compose the MATD of a Generalized Cylinder.

4.3.1 Topology of the MATD

As the reconstructed Discrete MAT is a discretization of the analogical MAT ([Pui98a]), here, the properties of the analogical MAT of a Generalized Cylinder have been analyzed and they have been extended to the discrete case.

Any point p of the MAT can be classified according to the type of tangency with the surfaces and the curves that compose the MAT ([Ver94]). Objects under consideration satisfy some topological and geometrical constraints: they are connected manifold objects, they have an interior with a finite volume and they have finite area. According to [Ver94], under these assumptions, the MAT points of these objects can be classified into seven groups (PI, PII, CI, CII, SI, SII, SIII).

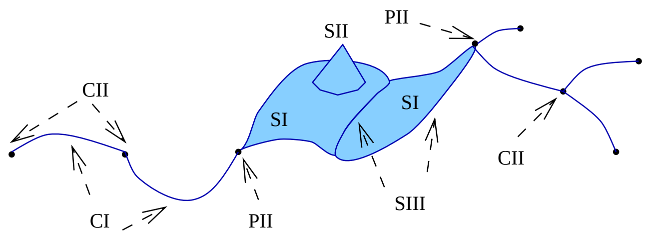

Figure 8: Taxonomy of the points of the MAT.

In the particular case of the Generalized Cylinders this taxonomy reduces to the type of points that form a linear MAT (see Figure 8):

- CI: p is a point of a curve of the MAT that has a continuous tangent.
- CII: p is a point of a curve of the MAT such that a finite number of tangent vectors to p exists, but p does not have a continuous tangent. p can be an end-point of the MAT or a final point of the curve.
- SI: p is a point of the surface of the MAT and the MAT has a continuous tangent plane at p.

- SII: p is an isolated singularity point of the surface of the MAT.
- SIII: p is a point of a curve of the MAT which is the intersection of two surfaces of the MAT or a limit curve of a surface of the MAT.
- PII: p belongs to a curve and to a surface of the MAT.

The PI points of general objects should not be considered because PI points are isolated points of the MAT, i.e, PI points occur when the object is a sphere.

In order to extend this taxonomy to the discrete case, it is necessary to state briefly the definitions of the environment and the wave. These definitions will allow to label every voxel of the discrete MAT with one of the possible types of the set $TAX = \{CI, CII, PII, SI, SIII\}$. This classification can be done locally at every voxel, according to the definitions specified and shown in Figure 9. It should be noted that in the discrete case, SII points, which are isolated singularities of a MAT surface, can be considered as particular cases of SI or degenerations to SIII points and therefore SII will not be treated separately.

Def. 2. Given a voxel v of the MATD and a direction $\bar{dir}$ perpendicular to a coordinate plane (i, j, k), $environment(v, \bar{dir})$ is defined as the intersection of the MATD with the plane, defined by its normal vector $\bar{dir}$ which passes through the next voxel to v on the direction $\bar{dir}$:

$$environment(v, \bar{dir}) = \{v' \in MATD \ / \ v' \cap plane\_voxels(\bar{dir}, v + \bar{dir}) \neq \phi\}$$

The secondary directions can be defined as the perpendicular direction of any of the coordinate planes (i, j, k) which are different to $\bar{dir}$.

Prop 1. *Given an environment*$(v, \bar{dir})$ *of the* $MATD$*, it can be splitted into at most* $N/2$ *6-connected sets:*

$$0 \leq \#6\_connected\_set(environment(v, \bar{dir})) \leq N/2$$

and N *is the size of an edge of the voxel set where the MATD is extracted.* [1]

Def. 3. Given a voxel v of the MATD and a direction $\bar{dir}$, $wave(v, \bar{dir})$ are the 6-connected sets of $environment(v, \bar{dir})$ which are 26-connected to v:

$$wave(v, \bar{dir}) = \{c \in environment(v, \bar{dir}) \ / \ \exists v' : v' \in c : v' \in neighbors_{26}(v)\}$$

Prop 2.

$$1 \leq \#(wave(v, \bar{dir})) \leq 5$$

Prop 3. *Every connected set of* $wave(v, \bar{dir})$ *of the* $MATD$ *fullfils that* $c \in wave(v, \bar{dir})$, $0 \leq \#c \leq N$.

[1] The notation $\#(set)$ identifies the number of the elements of the set. The type of the elements is the one specified into the set definition. For instance, $\#(environment(v, \bar{dir}))$ is the number of the voxels which belong to the environment, while $\#(wave(v, \bar{dir}))$ is the number of connected sets that compose the wave.

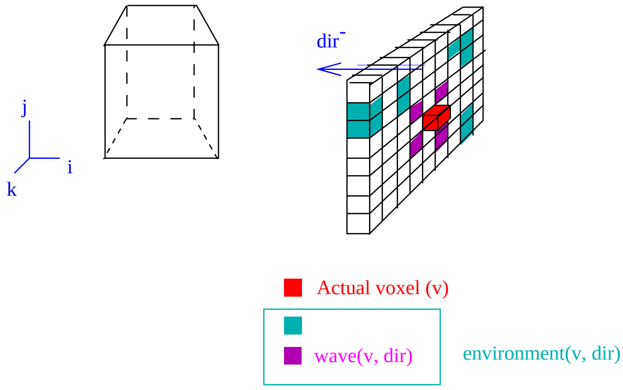

Figure 9: Concepts of $\bar{dir}$, $environment(v, \bar{dir})$ and $wave(v, \bar{dir})$.

The definition of the wave of a voxel of the $MATD$ can be generalized to the wave of a set of voxels. This generalization is used to analyze a wave of another wave:

Def. 4. Given a 6-connected set of voxels V of the MATD and a direction $\bar{dir}$, $wave(V, \bar{dir})$ is the set of connected sets of $environment(V, \bar{dir})$ that are 26-connected to V:

$$wave(V, \bar{dir}) = \{c \in environment(V, \bar{dir}) \;/\; \exists v' : v' \in c : v' \in neighbor_{26}(V)\}$$

The voxels of a wave can be classified into axis-type or surface-type by studying the projections of the wave.

The $projection_l$ of a voxel set, $\{(i, j, k)\}$, into the coordinate plane l is the set of voxels $\{(0, j, k)\}$ if l=i, $\{(i, 0, k)\}$ if l=j, $\{(i, j, 0)\}$ if l=k }.

Def. 5. Let c be a connected set of $wave(v, \bar{dir})$, $proj_1(c)$ and $proj_2(c)$ are defined as the sets of voxels in which c is projected according to the secondary directions.

$$\forall s : 1 \leq s \leq 2 : proj_s(c) = \{p \; voxel / p \in projection_{s_l}(c) \; with \; l = i, j, \; or \; k\}$$

Recalling that the discretization of a line in 3D has a maximum width of four voxels in its main direction and two voxels in any of its secondary coordinate plane axis (see Figure 10), a linear wave can be defined as a single wave of four voxels width and a maximum of two voxels in each secondary projection.

Def. 6. A *linear wave* is a wave $wave(V, \bar{dir})$ such that:

$$\begin{aligned} wave(V, \bar{dir}) = 1 \quad & \& \; c \in wave(V, \bar{dir}) : \#c \leq 4 \\ & \& \; \#proj_1(c) \leq 2 \;\&\; \#proj_2(c) \leq 2 \end{aligned}$$

Def. 7. Given a MATD and a direction $\bar{dir}$ a connected set of waves is *a linear set ($LS_{\bar{dir}}$)* if and only if all the waves of the set are linear and if they share the same direction.

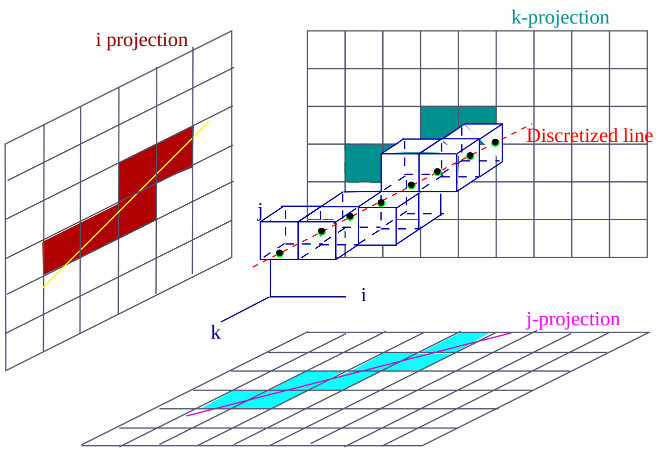

Figure 10: Projection of a discretized line.

A wave V of $LS_{\bar{dir}}$ is an interior wave, if $wave(V, \bar{dir}) \in LS_{\bar{dir}}$ & $wave(V, -\bar{dir}) \in LS_{\bar{dir}}$.

A wave V of $LS_{\bar{dir}}$ is an end-line of the Linear Set, if $wave(V, \bar{dir}) \notin LS_{\bar{dir}}$ $\|$ $wave(V, -\bar{dir}) \notin LS_{\bar{dir}}$. Obviously, one of them always belongs to $LS_{\bar{dir}}$, because V belongs to $LS_{\bar{dir}}$.

These definitions for linear waves can be extended to surface-waves.

Def. 8. A *surface-wave* is a wave $wave(V, \bar{dir})$ such that:

$$\begin{aligned} wave(V, \bar{dir}) = 1 \quad & \& \ c \in wave(v', \bar{dir}) : \#c > 4 \\ & \| \ \#proj_1(c) > 2 \ \| \ \#proj_2(c) > 2) \end{aligned}$$

Def. 9. Given a MATD and a direction $\bar{dir}$, a connected set of waves is *a surface set ($SS_{\bar{dir}}$)* if and only if all the waves of the set are surface-waves and if they share the same direction.

A wave V of $SS_{\bar{dir}}$ is interior to the Surface Set if $wave(V, \bar{dir}) \in SS_{\bar{dir}}$ & $wave(V, -\bar{dir}) \in SS_{\bar{dir}}$.

A wave V of $SS_{\bar{dir}}$ is an end-surface if $wave(V, \bar{dir}) \notin SS_{\bar{dir}}$ $\|$ $wave(V, -\bar{dir}) \notin SS_{\bar{dir}}$.

On the basis of these definitions, the taxonomy of the voxels of the MATD can be defined as follows:

- **CI voxels** belong to an inner wave of a Linear Set.

  Def. 10. A voxel v of the MATD is CI if and only if it $\exists v' \in MATD$ & $\exists dir : dir \in \{i, j, k\} : v \in wave(v', \bar{dir})$ & $\exists S :$ S is a Linear Set $: wave(v', \bar{dir})$ is an inner wave of S.

- **CII voxels** correspond to end-lines or modifications of the main direction of a line. Therefore, either their neighbor in a half direction of the line will be classified as a CI voxel and in the other half direction they will not have any neighbor, i.e. the number of waves from the voxel is zero (see case CII a or linear end-point in Figure 11) or they belong to two linear waves (see case CII b or linear elbow in Figure 11) or they will have more than two linear waves (see case CII c or linear branching in Figure 11).

Def. 11. A voxel v of the MATD is CII if and only if it $\exists dir : dir \in \{i,j,k\} : v \in wave(v', \bar{dir})$:

$$
\begin{array}{rll}
\exists! S : & S \text{ is a Linear Set } : & \text{CII a} \\
 & wave(v, \bar{dir}) \text{ is an end-line wave of } S. & \\
\exists! S_1, \exists! S_2 : & S_1 \text{ and } S_2 \text{ are Linear Sets } : & \text{CII b} \\
 & wave(v', \bar{dir}) \text{ is an end-line wave of } S_1 \text{ and of } S_2. & \\
\exists S_1 \ldots S_n : & n > 2 : \quad S_i \text{ are Linear Sets } : & \text{CII c} \\
 & wave(v', \bar{dir}) \text{ is an end-line wave of } S_i. &
\end{array}
$$

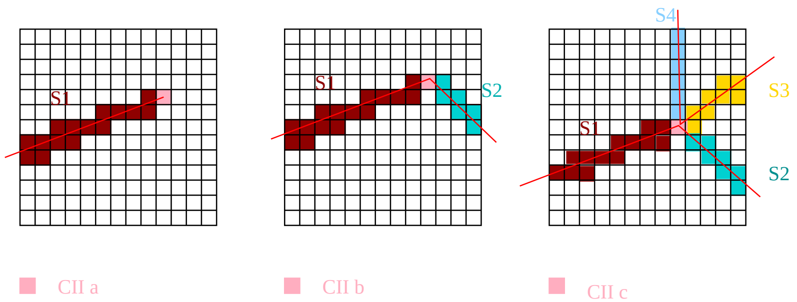

Figure 11: Topologies of the CII voxels.

- **SI voxels** belong to an inner wave of a Surface Set.

  Def. 12. A voxel v of the MATD is SI if and only if it $\exists dir : dir \in \{I,J,K\} : v \in wave(v', \bar{dir})$ & $\exists S$: S is a Surface Set: $wave(v', \bar{dir})$ is an inner wave of S.

  Prop 4. *The wave $wave(v', \bar{d_i})$ to which a SI-voxel v belongs has one and only one projection that fullfils that $\#proj_j(c) \leq 2$, where c is the only connected set that belongs to the wave.*

- **SIII voxels**, as CII voxels in the linear cases, correspond to end-surface, to changes of the main direction of a surface or to branchings of a surface. Therefore, either their neighbor in a half direction of the line will be classified as a SI voxel and in the other half direction they will not have any neighbor (see case SIII a or surface end-point in Figure 12) or they belong to two different surface waves (see case SIII b or surface elbow in Figure 12) or they will have more than two surface waves (see case SIII c or surface branching in Figure 12).

Def. 13. A voxel v of the MATD is $SIII$ if and only if it $\exists dir$: $dir \in \{I, J, K\} : v \in wave(v', \bar{dir})$:

$\exists! S$:	S is a Surface Set : $wave(v, \bar{dir})$ is an end-surface wave of S.	SIII a
$\exists! S_1, \exists! S_2$:	S_1 and S_2 are Surface Sets : $wave(v', \bar{dir})$ is an end-surface wave of S_1 and of S_2.	SIII b
$\exists S_1 \ldots S_n$:	$n > 2 : S_i$ are Surface Sets : $wave(v', \bar{dir})$ is an inner wave of S_i.	SIII c

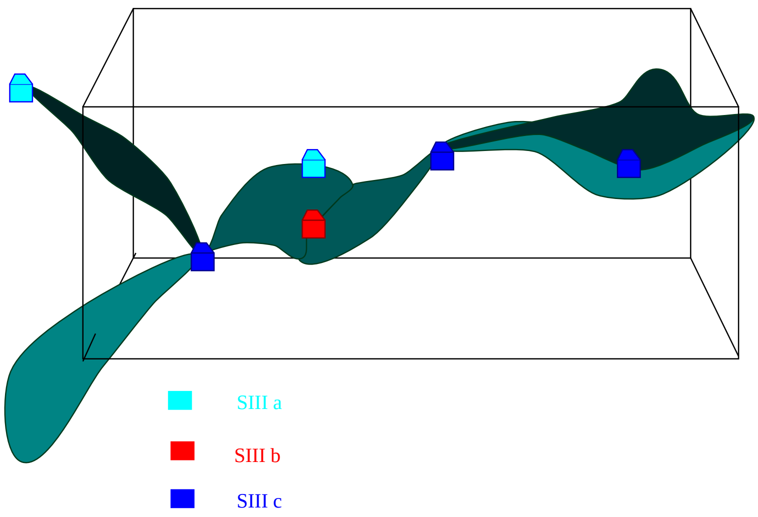

Figure 12: Topology of the SIII voxels.

- **PII voxels** are at the boundary between surface MATD and linear MATD. Two cases should be distinguished depending on the number of the lines and surfaces meeting at the point. PII voxels can be the meeting point of one surface wave and one linear wave (see case PII a in Figure 13) or they can be the connection point of more than one of such waves (see case PII b in Figure 13).

Def. 14. A voxel v of the MATD is PII if and only if it $\exists dir$: $dir \in \{I, J, K\} : v \in wave(v', \bar{dir})$:

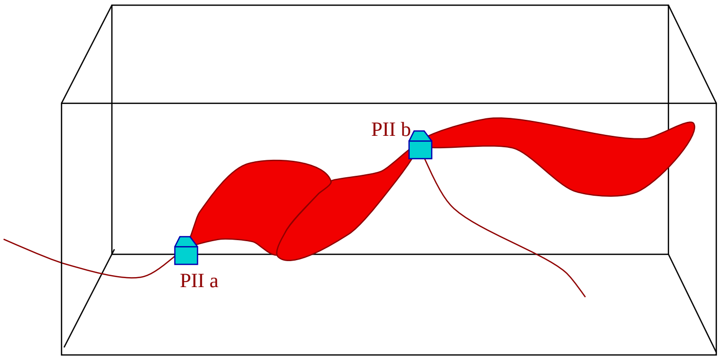

Figure 13: Topologies of the PII voxels.

$$
\begin{array}{lll}
\exists ! S_1, \exists ! S_2 : & S_1 \text{ is a Linear Set and} & \text{PII a} \\
& S_2 \text{ is a Surface Set } : & \\
& wave(v', \bar{dir}) \text{ is an end-surface wave of } S_1 & \\
& \text{and it is an end-line wave of } S_2. & \\
\exists S_1 \ldots S_n, \quad \exists L_1 \ldots L_m : & m \text{ or } n > 2 : S_i \text{ are Surface Sets and} & \text{PII b} \\
& L_j \text{ are Linear Sets} : & \\
& wave(v', \bar{dir}) \text{ is an end-surface wave of } S_i & \\
& \text{and it is an end-line wave of } L_j. &
\end{array}
$$

4.3.2 Labeling algorithm

The construction algorithm is based on a seed strategy that begins with a voxel of the MATD and a main direction associated at this voxel. A study of the projections of its wave classifies the voxels into the different categories above defined and constructs incrementally the graph model. This wave is the new seed for the next step of the algorithm. The validity of this seed strategy is obviously a consequence of the locality of the calculations.

Thus, the discrete MAT can be splitted into segments delimited with points typified as CII a, CII b, CII c, SIII b, SIII c, PII a and PII b, this means, with boundary points between various curves, between curves and surfaces and between various surfaces.

It is possible to distinguish between two cases of SIII c (Figure 14): real branching of the surface (SIII c1) or book branching (SIII c2). In the case of real branching the Surface Sets share only a single end-surface wave. Besides, if more than one end-surface wave of the Surface Sets are shared, there is a book branching case.

The labels of the graph model can be determined according to the following considerations. First, a real branching of a vessel is defined by every point which is typified as CIIc, PIIb o SIIIc1. Moreover, all set of points CI, CIIa and CIIb are labeled as a normal segment of a vessel. Instead the changes

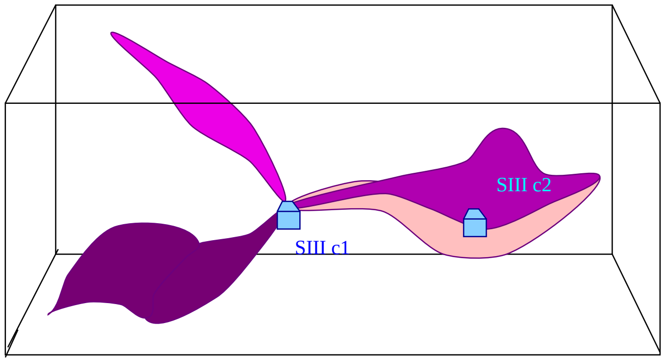

Figure 14: Cases SIII c1 and SIII c2.

of direction or the end-points of a normal segment are not labeled explicitly and thus their associated information must be stored. Therefore, a change of direction can be detected at a CIIb voxel while an end-point of a segment is a CIIa point. Finally, a non-normal segment is labeled by the sets of the PIIa, SI, SIIIa, SIIIb and SIIIc2 points. In a non-normal segment, the SIIIa points detect some change of the main direction.

To distinguish between aneurysms and stenoses in the non-normal segments, the length of the segment and the diameters of the MATD must be computed and compared according to the physicians metrics. However, short vessel branches may be confused with aneurysms and in vessels of small diameter, stenoses and aneurysms, being dual, may also be misclassified.

4.4 Algorithm of construction of the surface model

In order to obtain the surface information of the model it is necessary to define an axis of the Generalized Cylinder and its associated cross sections. These cross sections are defined at some relevant points of the axis.

Taking into account the results of the last section, a vectorization algorithm of the labeled MATD that obtains the main axis of the model is next proposed (see Figure 15).

It can be considered that the MATD is divided into regions bounded by CII a, CII b, CII c, SIII b, SIII c, PII a i PII b voxels (see section 4.3.2). In each region, the voxels of the MATD can be classified into two sets: Linear Sets and Surface Sets.

The Linear Sets of the MATD are fitted by CII a, CII b, CII c, PII a and PII b voxels. The core of the algorithm is the search of a straight line going through CI voxels that belong to a Linear Set. If it is not possible to match a single line that crosses all CI voxels of the region, the algorithm divides the line into two segments in order to obtain a piecewise linear approximation of the curve. The line is regularly sampled at a given resolution and a set of cross sections are computed at the sample points. A cross section is obtained by intersecting the plane defined by the main direction of the axis with the boundary voxels of the blood vessels. An intersection of a voxel with a plane gives a polygon which is approximated by its central point. Thereby, the cross section is composed by the full ordered set of these central points.

The Surface Sets of the MATD are bounded by SIII b, SIII c1, PII a and PII b voxels. The basic idea of the algorithm is to define a straight line that crosses SIII c2 points and SI points. The SIII c2 points are considered similarly to the CI points of the linear set. The main direction of SI points is computed as the main direction of their waves. The algorithm navigates through the connected SI points and it computes an approximate straight line. The SIII b points produce changes in the direction of the straight line, as CII b points do in the linear case. Finally, the cross sections associated to the relevant points of the straight line of the surface are computed in the same way as in the linear case.

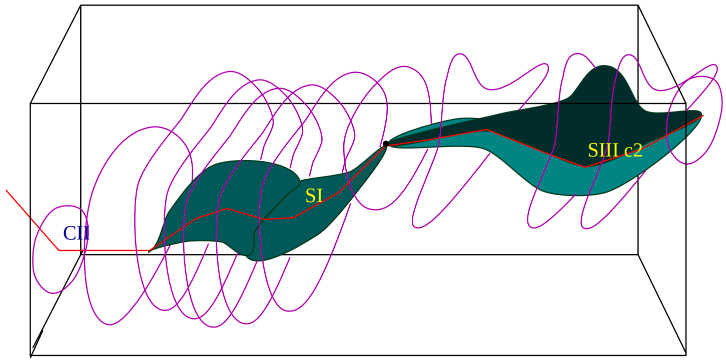

Figure 15: Axis of the Generalized Cylinder and the MATD.

Therefore, all the computations of the surface construction algorithm are local to a region and they can be performed with a seed process with a bigger granularity than the seed process which labels the voxels.

4.5 Construction of the volume model

In this section the construction of the volume representation scheme defined in section 3 is presented.

A new scalar property is defined in the initial volume model, that identifies the elements of the graph to which the voxel belongs. A voxel usually belongs to a single element, except voxels which are at the boundary between various elements that are marked as belonging to all of them. The value of this n-dimensional property at each voxel is actualized during the process of construction of the symbolic model (see 4.3.2).

This new voxel model is run-length encoded([Lac95]). The construction of the encoded volume model is performed in a post-process in which each compact set of voxels is labeled with the identifier of the element of the graph to which it corresponds. During this traversal, the voxels corresponding to each segment are also stored in the symbolic graph taking into account that every voxel of the model has already been classified with regard to the surface. The cost of the algorithm is directly linear with the input voxel model size. However it should be noted that it is a pre-process cost that speeds up the operations which are performed afterwards on the model.

4.6 Evaluation

The analysis of the cost of the algorithm has been done taking into account the following property: if A1 is a seed algorithm imbricated into another seed algorithm A2, being g_1 and g_2 their respective granularities such that $g_2 = N \times g_1$, and being their cost functions at each step $O(k_1)$ i $O(k_2)$, then the total cost of A2 is $O(k) = O(p \times N \times k_1)$, being p the number of passes of the granule of A2.

Let N be the number of voxels of the input data and $k_1 \times N$ be the number of "vascular" voxels, with $0 \leq k_1 \leq 0.5$. The maximal diameter of the vessels is d and it is assumed that the Discrete Medial Axis occupies $k_2 \times k_1 \times N$ voxels, with $0 \leq k_2 \leq 1$.

Starting from a voxel of the MATD, the Medial Axis of the vessels is constructed in a single pass. The computing cost of the Distance Map is constant per-voxel and it has a value of O_{DM}. The analysis of the properties of the boundary of the sphere that represents the Distance Map is O_{MAD}, which is also constant per-voxel. Finally the labeling of the Distance Map voxels is constant: O_{etiq}.

Simultaneously, at a higher level of granularity, the symbolic model and the surface model are constructed and the voxels which are interior to each feature of the symbolic model are marked. These processes have constant costs per granule which in the worse case has a value of one. Therefore, the total cost of the seed process is :

$$O_{germen}(N, k_1, k_2, d) = k_2 \times k_1 \times N \times [O_{DM} + O_{MAD} + O_{etiq}]$$

This is, it has a linear cost with the number of voxels that compose the MATD. This is considerably less than other methods that analyze the whole voxel model, because the vessels occupancy is at most a 20% of the voxels and the MATD is at most of the same size than the vessels.

The run-length encoding of the voxel model is performed in a post-process and saved in the symbolic model. The cost of this post-process is linear in relation to the number of voxels that belong to the vascular map.

The limitations of the method are related to the capture process and the nature of the vessels:

- Capture errors: two vessels passing through the same voxel are considered as one. Accordingly, two vessels which pass through adjacent voxels without an external voxel in between, are treated as a single one.
- Misclassification: Some features may be misclassified because the physicians metrics may be ambiguous in some cases. As an example, it is difficult to give an exact criterion for the distinction between aneurysms and small branches. Physicians distinguish them on the basis of their experience and knowledge taking into account the coincidence of various facts, hardly expressible.

- Some branchings are undetected until an external voxel enables to separate the branches.

It should be noted however that the misclassifications are not frequent. They are related to the type of data and not attributable to the algorithm itself. They can be corrected by using an interactive editor.

5 Conclusions and Future Work

The main contribution of this report is the proposal of a representation scheme for blood vessels, of their surface as well as their volume. The model is hybrid: it stores symbolic information on the topology and geometry as well as volume and surface data. These characteristics provide flexibility and enable the realization of all the physicians requirements in a Computed Assisted Neurovascular System.

An algorithm of construction of the model from a set of images, based on the extraction of the discrete MAT and exploiting a seed strategy has been proposed. The evaluation of its cost of the algorithm shows that it is considerably less than other methods.

In addition, the model can be visualized using different approaches surface-based, volume-based or mixed. This is addressed in the report [Pui98b].

References

[AOUK87] K. Anjyo, T. Ochi, Y. Usami, and Y. Kawashima. A practical method of constructing surfaces in three-dimensional digitized space. *The Visual Computer*, 3(1):4–12, February 1987.

[BGSC85] C. Barillot, B. Gibaud, J. Scarabin, and J. Coatrieux. 3d reconstruction of cerebral blood vessels. *IEEE Computer Graphics and Applications*, 5(12):13–19, December 1985.

[BJN+94] P. Brunet, R. Juan, I. Navazo, A. Puig, J. Sole, and D. Tost. Modeling and visualization trough data compression. *Data Visualization*, 1994.

[Boi85] J.D. Boissonnat. Surface reconstruction from planar cross section. *Proceedings IEEE Computer Society Conference on Computer Vision and Pattern Recognition*, pages 393–397, 1985.

[CLKJ90] H.C. Cline, W.E. Lorensen, R. Kikinis, and F. Jolesz. Three-dimensional segmentation of mr images of the head using probability and connectivity. *Journal of Computer Assisted Tomography*, 14(6):1037–1045, November/December 1990.

[CP92] K. Chin-Purcell. Bob: Brick of bytes. *AHPCRC, Minnesota SuperComputer Center (Software for Silicon Graphics)*, 1992.

[EDKS94] H.H. Ehricke, K. Donner, W. Koller, and W. Straber. Visualization of vasculature from volume data. *Computer and Graphics*, 18(3):395–406, 1994.

[EL90] H.H. Ehricke and G. Laub. Combined 3d-display of cerebral vasculature and neuroanatomic structures in mri. *3D Imaging in Medicine: Algorithms, Systems and Applications*, pages 229–239, 1990.

[FR92] S. Flesia and M. Roche. 3d reconstruction of generalized cylinders from biplane projection. *Computer and Graphics*, 16:167–173, 1992.

[GCCC91] M. Garreau, J.L. Coatrieux, R. Collorec, and C. Chardenon. A knowledge-based approach for 3d reconstruction and labeling of vascular networks from biplane angiographic projections. *IEEE Transactions on Medical Imaging*, 10:122–131, June 1991.

[GKJ90] G. Gerig, R. Kikinis, and F.A. Jolesz. Image processing of routine spin-echo mr images to enhance vascular structures: Comparison with mr angiography. *3D Imaging in Medicine: Algorithms, Systems and Applications*, pages 121–132, 1990.

[GKS+93] G. Gerig, Th. Koller, G. Székely, Ch. Brechbühler, and O. Kübler. Symbolic description of 3-d structures applied to cerebral vessel tree obtained from mr angiography volume data. *Proceedings of the 13th International Conference on Information Processing in Medical Imaging, Springer-Verlag, New York/Berlin*, pages 94–111, 1993.

[GS95] A. Savopoulos G. Sakas, M. Grimm. Optimized maximum intensity projection (mip). *6th Eurographics Workshop on Rendering*, pages 81–93, June 1995.

[HBP+90] K.H. Hohne, M. Bomans, A. Pommert, M. Riemer, C. Schierds, U. Tiede, and G. Wiebecke. 3d visualization of tomographic volume data using the generalized voxel-model. *The Visual Computer*, 6(1):28–36, February 1990.

[HL79] G.T. Herman and H.K. Liu. Three-dimensional display of human organs from computed tomograms. *Computer Graphics and Image Processing*, 9(1):1–21, 1979.

[HMS95] W. Heidrich, M. McCool, and J. Stevens. Interactive maximum projection volume rendering. *Proceedings of the IEEE Volume Visualization 95*, pages 11–18, October 1995.

[HTL+89] X. Hu, K.K. Tan, D.N. Levin, S.G. Galhorra, C.A. Pelizzari, G.T.Y. Chen, R.N. Beck, C.T. Chen, and M.D. Cooper. Volumetric rendering of multimodality, multivariable medical imaging data. *Proceedings of Chapel Hill Workshop on Volume Visualization*, pages 45–49, 1989.

[KPL94] M/S. Kim, E.J Park, and H.Y. Lee. Modelling and animation of generalized cyllinders with variable radius offset space curves. *The Journal of Visualization and Computer Animation*, 5:189–207, 1994.

[KTS88] K. Kitamura, J.M. Tobis, and J. Sklansky. Estimating the 3d skeletons and traverse areas of coronary arteries from biplane angiograms. *IEEE Transactions on Medical Imaging*, 7:173–187, September 1988.

[Lac95] P. Lacroute. Fast volume rendering using a shear-warp factorization of the viewing transformation. Technical report, Departments of Electrical Engineeering and Computer Science, Stanford University, Setember 1995.

[LK94] T.C. Lee and R.L. Kashyap. Building skeleton models via 3d medial surface/axis thinning algorithms. *CVGIP: Graphical Models and Image Processing*, 56(6):462–478, November 1994.

[Man88] M. Mantyla. *An Introduction to Solid Modeling*. Computer Science Press, 1988.

[MMD96] Y. Masutani, K. Masamune, and T. Dohi. Region-growing based feature extraction algorithm for tree-like objects. *Proceedings of 4th International Conference Visualization in Biomedical Computing, Hamburg, Germany*, pages 161–171, September 1996.

[MPSY97] T. Maekawa, N.M. Patrikalakis, T. Sakkalis, and G. Yu. Analysis and applications of pipe surfaces. *Computer Aided Geometric Design*, 1997.

[NPT93] I. Navazo, A. Puig, and D. Tost. Research trend in volume modeling. *Report LSI-93-35-R*, 1993.

[Pui98a] A. Puig. Discrete medial axis transform for discrete objects. *Report LSI-98-22-R, Polytechnical University of Catalunya, Spain*, 1998.

[Pui98b] A. Puig. Visualization of cerebral blood vessels. *Report LSI-98-20-R, Polytechnical University of Catalunya, Spain*, 1998.

[Req80] A. Requicha. Representations for rigid solids: Theory, methods and systems. *Computing Surveys*, 12(4), December 1980.

[Ros85] J.R. Rossignac. *Blending and Offsetin Solid Models*. PhD thesis, University of Rochester, Production Automation Project Technical Memorandum, 54, July 1985.

[SFTPR90] D. Saint-Felix, Y. Trousset, C. Picard, and A. Rougee. 3d reconstruction of high contrast objects using multi-scale detection / estimation scheme. *3D Imaging in Medicine*, pages 145–158, 1990.

[SVD+91] P. Suetens, R. Verbeeck, D. Delaere, J. Nuyts, and B. Bijnens. Model-based image segmentation:methods and applications. *Proceedings of 3rd Conference on Artificial Intelligence in*, 44, 1991.

[Udu92] J.K. Udupa. Applications of digital topology in medical three-dimensional imaging. *Topology and its Applications*, 46:181–197, 1992.

[Ver94] P.J. Vermeer. Medial axis transform to boundary representation conversion. *PhD Thesis, Purdue University*, May 1994.

[VVB+94] D. Vandermeulen, R. Verbeeck, L. Berben, D. Delaere, P. Suetens, and G. Marchal. Continuous voxel classification by stochastic relaxation: Theory and application to mr imaging and mr angiography. *Internal Research Report, Medical Imaging Research Lab, ESAT, Belgium*, 1994.

[VVM+93] R. Verbeeck, D. Vandermeulen, J. Michiels, P. Suetens, G. Marchal, J. Gybels, and B. Nuttin. Computer assited stereotactic neurosurgery. *Image and Vision Computing Volume*, pages 468–485, October 1993.

[WHH+93] S.A. Wood, J.D. Hoford, E.A. Hoffman, E. Zerhouni, and W.A. Mitzner. Quantitative 3-d reconstruction of airway and pulmonary vascular trees using hrct. *SPIE Proc. Biomedical Image Proc. Comput. Vision*, 1905:316–323, 1993.

[WW97] J. Williams and L. Wolff. Analysis of the pulmonary vascular tree using differential geometry based on vector fields. *Computer Vision and Image Understanding*, 65(2):226–236, February 1997.

[ZJP94] C. Zahlten, H. Jurgens, and H.O. Peitgen. Reconstruction of branching blood vessels from ct-data. *Proceedins of Rostock*, 1994.

[Zui96] K.J. Zuiderveld. Vr in radiology - first experiences at the university hospital utrecht. *ACM Computer Graphics*, pages 47–48, November 1996.